

## Modelling a solid-state fluidized bed fermenter for Ethanol production with *S. cerevisiae*

L. Röttenbacher, Burghausen, M. Schöbler, Hamburg, and W. Bauer, München

**Abstract.** A model is proposed to describe the performance of a new type of fermenter for ethanol production, the fluidized bed gas-solid fermenter, with respect to scaling-up effects. Based on the fact that in the fluid bed the substrate is not supplied continuously to each particle, two scale-up parameters are derived, circulation time  $\tau$  and specific substrate supply  $\Delta m_{G,P}$ , which are shown to influence reactor efficiency significantly. The validity of the model is checked by comparing the calculated yield coefficients for ethanol, cell mass and carbon dioxide to the results of fermentation experiments performed under aerobic conditions in a laboratory-scale reactor and a semi-technical fermenter.

### List of symbols

$A$	$m^2$	bed surface
$A_s$	$m^2$	bed surface to which substrate is supplied
$c_i$	$kg/m^3$	concentration of species $i$
$C_{O_2,0}$	$kg/m^3$	concentration of oxygen in water at saturation
$D_i$	$m^2/s$	diffusion coefficient of species $i$
$E$	$J/mol$	activation energy
$H$	$m$	expanded bed height
$k_m$	$h^{-1}$	maintenance coefficient
$K_{S,v}$	$kg/m^3$	Michaelis-Menten constant for ethanol production
$K_{S,\mu}$	$kg/m^3$	Michaelis-Menten constant for growth on glucose
$M_i$	$g/mol$	molecular weight of species $i$
$m_i$	$g$	mass of species $i$
$\dot{m}_{G,v}$	$kg/(m^3 \cdot h)$	specific glucose feed
$\dot{m}_i$	$g/s$	mass flow of species $i$
$p_i$	$mbar$	partial pressure of species $i$
$r$	$m$	radial distance
$R$	$m$	pellet radius
$t$	$s$	time
$T$	$K$	temperatur
$u$	$m/s$	velocity
$V_a$	$m^3$	pellet volume, where oxygen is available
$V_p$	$m^3$	pellet volume
$V_s$	$m^3$	solid volume; total yeast volume
$X$	$kg/m^3$	density of dry mass inside the pellet
$Y_{i/j}$		yield coefficient between species $i$ and $j$
$\bar{v}_b$		mean bubble gas holdup
$\epsilon_{mf}$		bed porosity at minimum fluidization
$\epsilon_p$		particle porosity
$\eta_{ws}$		efficiency factor for fluid bed fermenter
$\mu_G$	$h^{-1}$	spec. growth rate on glucose
$\mu_E$	$h^{-1}$	spec. growth rate on ethanol

$v$	$h^{-1}$	spec. ethanol production rate
$\rho$	$kg/m^3$	density
$\sigma_E$	$h^{-1}$	spec. oxygen consumption rate
$\tau$	$s$	circulation time
$\Phi$		Thiele module

### Subscripts

$b$	bubble
$C$	carbon dioxide
$dw$	dry weight
$E$	ethanol
$G$	glucose
$g$	gas
$O_2$	Oxygen
$p$	particle
$s$	solid
$st$	stationary
$W$	water
$Y$	yeast

## 1 Introduction

Up to now fluidized bed technology has been applied to many operations, including chemical, pharmaceutical and food processing. An entirely new way to use gas/solid fluidization is the application to biocatalysed reactions, such as the production of glutathion [1], single cell protein [2, 3] or ethanol [4, 5] by the yeast *saccharomyces cerevisiae*.

In the gas/solid fluid bed fermenter small pellets of pressed baker's yeast are fluidized by air or nitrogen. The substrate is fed continuously by two-phase nozzles. In the case of ethanol production this reactor offers the following advantages compared to conventional batch techniques:

- high cell density,
- small product inhibition, as the ethanol produced is continuously stripped by the fluidizing gas,
- no loss of sugar, as only volatile products leave the reactor,
- biological heat can be used for evaporation of water, so no external cooling is necessary.

Problems to be overcome are the control of the fluidization behaviour, which can be achieved by optical sensors [6] and the accumulation of undesired substances.

**2 Reactor model**

A model to describe the performance of the fluid bed fermenter with respect to scaling-up problems has to take into account not only the reaction kinetics, but also the influence of reactor diameter  $d_r$ , bed height  $H$ , and gas velocity  $u$  (see Fig. 1).

The model used is based on the fact that in the fluid bed fermenter substrate is not supplied continuously to a single particle, but only when it is passing the spraying zone of the nozzle. Between two spraying events the particle behaves like a little batch reactor. The assumption is made that there is a certain mean time interval  $\tau$  between two spraying events and that the quantity of glucose fed to the particle  $\Delta m_{G,P}$  is constant. The circulation time is coupled with the mixing behaviour of the system and therefore depends to a large degree on the scale of the reactor. The specific substrate supply  $\Delta m_{G,P}$  is limited by agglomeration effects and therefore depends on the spraying density of the nozzle as well as on the mixing quality of the reactor. The aim of our study was to show that the effectiveness and therefore the productivity of a given reactor can be calculated from these two parameters.

*2.1 Calculation of circulating time  $\tau$*

The calculation of the circulation time is based on the mechanism of bubble induced solids' transport, which means that in fluidized beds of particles larger than 100  $\mu\text{m}$  the upward flow of solids is solely caused by the action of rising bubbles [7].

Thus the circulation time can be calculated using the solids mass balance for the whole reactor (see Fig. 2) for a given bed height  $H$  and surface to which substrate  $A_S$  is fed according to Eq. (1) [8]

$$\tau = \frac{H}{\bar{u}_b} \left( \frac{1 - \bar{\epsilon}_b}{\epsilon_b \cdot f} + 1 \right) \cdot \frac{A}{A_S} \tag{1}$$

The values for the mean bubble gas hold-up  $\bar{\epsilon}_b$  and the mean bubble rise velocity  $\bar{u}_b$  in Eq. (1) are derived from empirical correlations for the local values of this parameters according to [9].  $f$  is a factor describing the amount of solids carried upward by the bubbles compared to total bubble volume. According to Rowe [7]  $f$  is about 0.6. For a given circulation time, the specific substrate supply  $\Delta m_{G,P}$  can then be calculated from the feed balance:

$$\Delta m_{G,P} = \frac{\dot{m}_G \cdot \tau}{V_S} \tag{2}$$

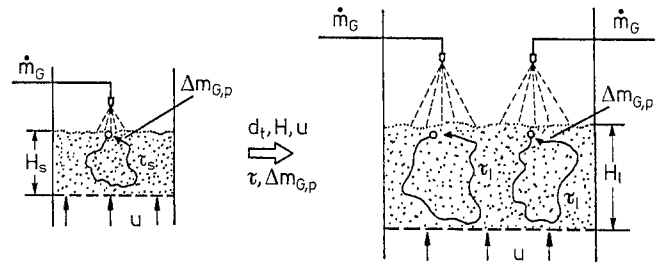


**Fig. 1.** Scale-up model for the fluid bed fermenter

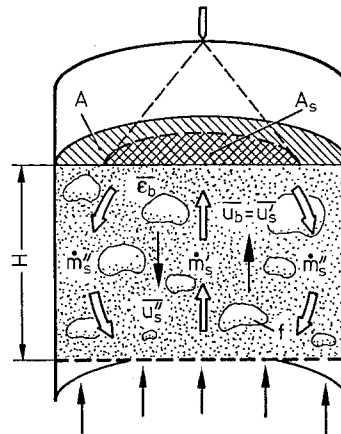


**Fig. 2.** Solids mixing in a gas/solid fluidized bed

*2.2 Ethanol production of a single pellet in the fluid bed*

Figure 3 schematically shows the metabolism of a single pellet between two spraying events. The influence of circulation time and specific substrate supply on ethanol production rate and yield is illustrated by the picture on the right hand side of Fig. 3, showing schematically the ethanol production rate on the pellet surface. Directly after the spraying event the sugar concentration on the pellet surface is very high, resulting in maximum ethanol production rate. For aerobic conditions ethanol production is always smaller than for anaerobic conditions due to growth and respiration. During the circulation the sugar concentration at the pellet surface decreases as glucose diffuses into the pellet and is partly consumed. So ethanol production falls according to a Michaelis-Menten type kinetics. For a certain critical sugar concentration  $C_{G, \text{crit}}$  the ethanol production rate under aerobic conditions equals the consumption for growth and respiration ( $t = \tau_2$  in Fig. 3), so  $\dot{m}_E$  becomes zero. For longer circulation times (e.g.  $\tau_3$  in Fig. 3) part of the ethanol produced may be reconsumed,  $\dot{m}_E$  becomes negative, resulting in a decrease of ethanol yield.

The quantity of alcohol produced by one particle during one circle can be calculated by integration (see Fig. 3). It is obvious that only for short circulation times high production rates resp. high productivities may be achieved.

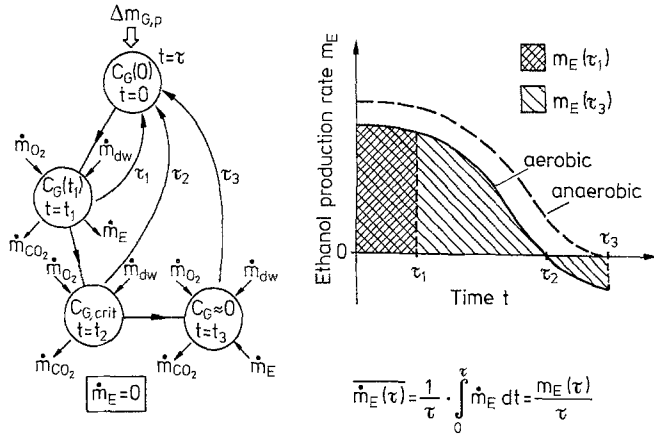


Fig. 3. Ethanol production of a single particle in the fluidized bed

Table 1. List of kinetic parameters

$v_{max}$	$= 6.15 \cdot 10^9$	$h^{-1}$
$E_v$	$= 57.6$	$kJ/mol$
$K_{S,v}$	$= 0.59$	$kg/m^3$
$\mu_{G,max}$	$= 1.18 \cdot 10^{10}$	$h^{-1}$
$E_{\mu,G}$	$= 61.5$	$kJ/mol$
$K_{S,\mu}$	$= 0.4$	$kg/m^3$
$\sigma_{E,0}$	$= 1.2 \cdot 10^{11}$	$h^{-1}$
$E_{\sigma,E}$	$= 70$	$kJ/mol$
$\mu_{E,0}$	$= 2.48 \cdot 10^3$	$h^{-1}$
$E_{\mu,E}$	$= 24.6$	$kJ/mol$
$k_m$	$= 0.012$	$h^{-1}$

### 3 Material balances

For an exact description of the reaction process inside the pellet mass transfer into the particle has to be taken into consideration, especially in the case of glucose. The non-stationary sugar balance inside the particle, which is considered to be a sphere is given by Eq. (3) together with initial values and boundary conditions of the nonlinear, partial differential equation:

$$\frac{\partial C_G}{\partial t} = D_G \left( \frac{\partial^2 C_G}{\partial r^2} + \frac{2}{r} \frac{\partial C_G}{\partial r} \right) - \frac{X}{\epsilon_p} \left( \frac{M_G}{2M_E} v(C_G) + \frac{M_G}{M_Y} \mu_G(C_G) + k_m \right). \quad (3)$$

Initial values:

$$C_G(r, 0) = \begin{cases} C_{G,0} & \text{for } r = R \\ 0 & \text{for } r \neq R \end{cases} \quad (3a)$$

Boundary conditions:

$$r = 0: \frac{\partial C_G}{\partial r} = 0 \quad (3b)$$

$$\frac{\partial C_G}{\partial t} = \frac{4\pi R^2 \cdot C_{G,0} \cdot D_G}{\Delta m_{G,P}} \cdot \frac{\partial C_G}{\partial r} \quad \text{for } t \neq n \cdot \tau \quad n = 0, 1, 2, 3$$

$r = R$ :

$$C_G(R, t) = C_{G,0} \quad \text{for } t = n \cdot \tau \quad (3c)$$

As in the fluid bed fermenter product inhibition can be neglected the specific ethanol production rate  $v$  and the specific growth rate on glucose  $\mu_G$  are given by Michaelis-Menten kinetics with a temperature dependence according to Arrhenius:

$$v(C_G) = v_{max} \cdot C_G / (K_{S,v} + C_G) \cdot \exp(-E_v/RT). \quad (4)$$

$$\mu_G(C_G) = \mu_{G,max} \cdot C_G / (K_{S,\mu} + C_G) \cdot \exp(-E_{\mu,G}/RT). \quad (5)$$

All the kinetic parameters needed for calculation were derived from experiments in a stirred tank reactor and are summarized in Table 1.

Equation (3) was solved by numerical methods, using an implicit difference method with a regulation of time steps using small radial steps near the pellet surface, where the steepest gradients occur. For each  $t = n \cdot \tau$  the surface concentration was corrected according Eq. (3c), simulating a new substrate supply.

As according to the model the mean circulation time is assumed to be constant for all particles, the steady state of the whole reactor is reached, when the concentration profiles at the end of two following circles are equal, i.e.:

$$C_G(r, t) = C_G(r, t - \tau). \quad (6)$$

Figure 4 shows examples for calculated sugar profiles inside the pellet at stationary conditions for the whole fermenter. The influence of circulation time and specific substrate supply on the concentration profile is obvious as only for short  $\tau$  and high  $\Delta m_{G,P}$  (Fig. 4a) the whole pellet is supplied with glucose. Combinations of circulation time and specific glucose supply as those in Fig. 4b and 4c would not only result in a decrease in productivity but also cause problems at long time fermentation such as cell lysis. For a given sugar profile the balance equations for ethanol, carbon dioxide and cell mass can be solved by integrating over the pellet volume  $V_p$  and circulation time. The yield coefficient for each species can then be calculated by dividing these values by the amount of sugar supplied at one spraying event, so:

Ethanol:

$$Y_{P/S,th} = \frac{X \left[ \int_0^\tau \int_{V_p} v(C_G) dV_p dt - V_a \cdot (3M_E \cdot \mu_E / M_{Y,dw} + M_E \cdot \sigma_E / 3M_{O_2}) \tau \right]}{\Delta m_{G,P} \cdot V_p} \quad (7)$$

Carbon dioxide:

$$Y_{C/S,th} = \frac{X \left[ \frac{M_C}{M_E} \int_0^\tau \int_{V_p} v(C_G) dV_p dt + V_a \cdot (2M_C \sigma_E \tau / 3M_{O_2}) \right]}{\Delta m_{G,P} \cdot V_p} \quad (8)$$

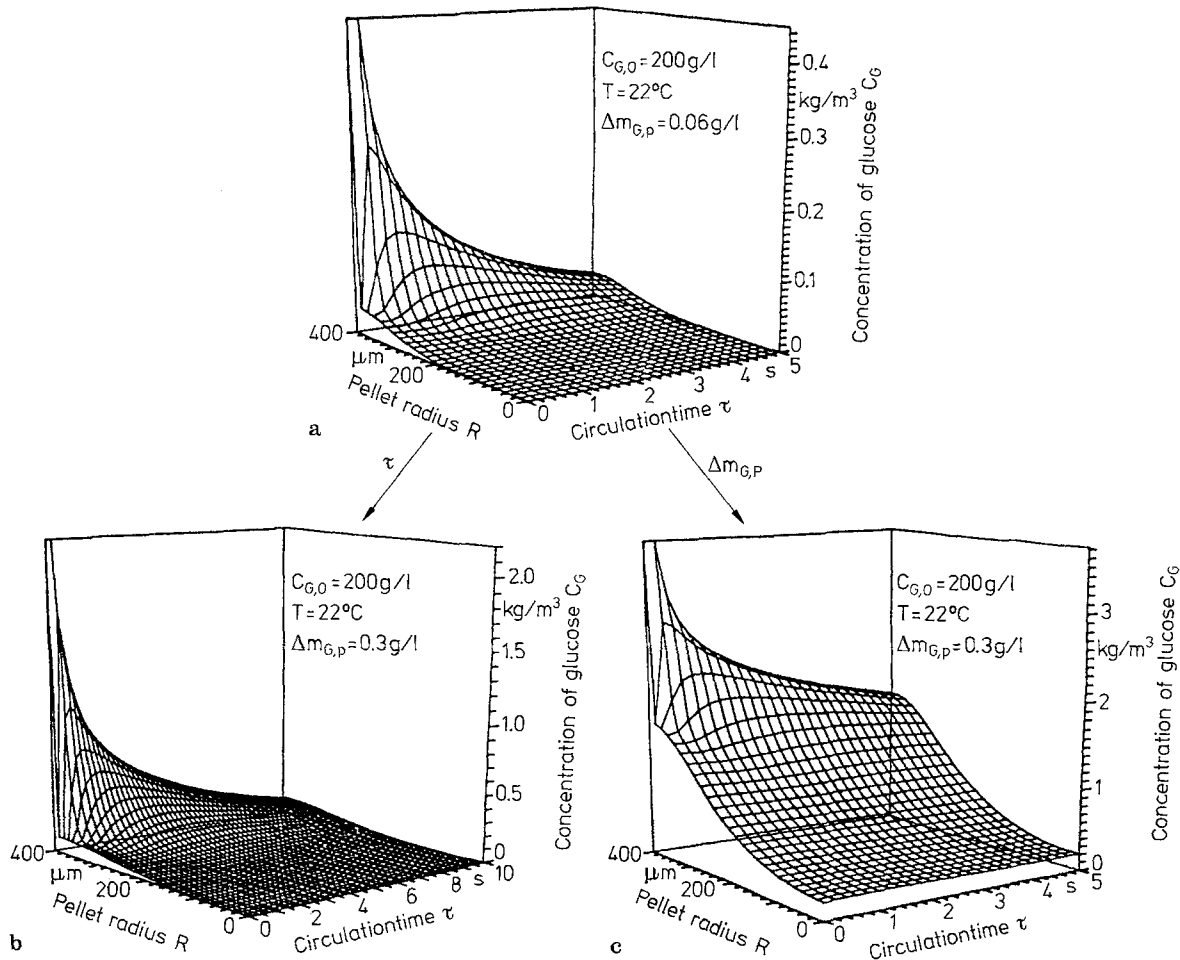


Fig. 4a-c. Influence of circulation time and specific substrate supply on the sugar concentration inside a pellet

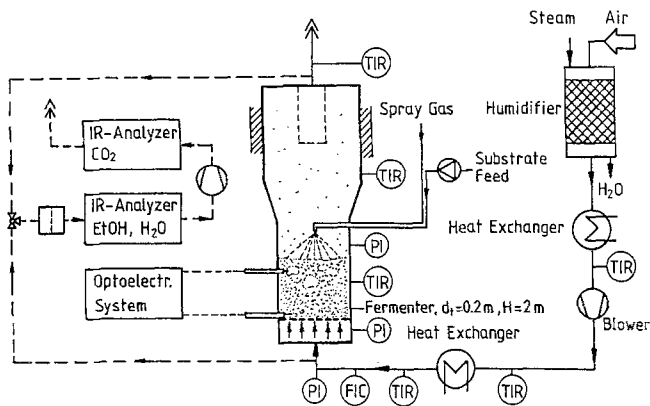


Fig. 5. Laboratory scale fluidized bed gas/solid fermenter

Cell mass:

$$Y_{X/S,th} = \frac{X \left[ \int_0^\tau \int_{V_p} \mu_G(C_G) dV_p dt + V_a \cdot \mu_E \cdot \tau \right]}{\Delta m_{G,P} \cdot V_p} \quad (9)$$

Equation (7)–(9) are derived for the assumptions that there are no concentration gradients for ethanol and carbon dioxide inside the pellet and that the rate of

growth on ethanol  $\mu_E$  and the oxidation rate of ethanol  $\sigma_E$  can be described by zero order reactions Eqs. (10) and (11) taking place only in the aerobic part of the pellet  $V_a$ .  $V_a$  may be calculated from oxygen balance [8] according to Eqs. (12) and (13):

$$\sigma_E = \sigma_{E,0} \cdot \exp[-E_{\sigma,E}/R \cdot T] \quad (10)$$

$$\mu_E = \mu_{E,0} \cdot \exp[-E_{\mu,E}/R \cdot T] \quad (11)$$

$$V_a = (4\pi R^3/3) \cdot [1 - (1 - 6/\Phi^2)^{3/2}] \quad (12)$$

$$\Phi = R[X \cdot \sigma_E / (D_{O_2} \cdot C_{O_2,0})]^{0.5} \quad (13)$$

#### 4 Fermentation experiments

To check the model the theoretically derived yield coefficients (Eqs. (7)–(9)) had to be compared with the results of fermentation experiments in the fluid bed fermenter.

##### 4.1 Apparatus and experimental procedure

Two reactors of different size were used for the experiments. A laboratory scale fluid bed with 20 cm diameter

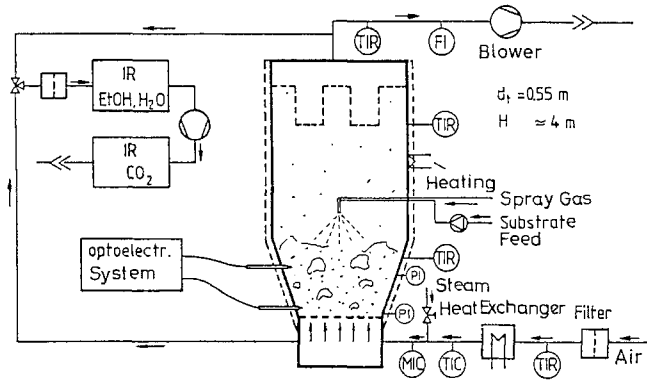


Fig. 6. Semi-technical fermenter; Glatt WSG 15

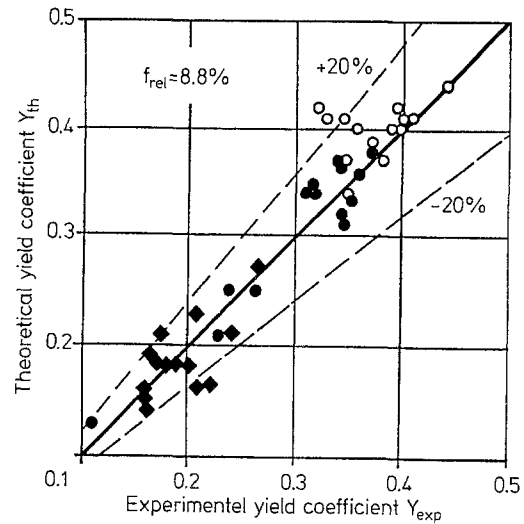


Fig. 9. Comparison of theoretical and experimental yield coefficients; Ethanol, Cell mass, Carbon dioxide

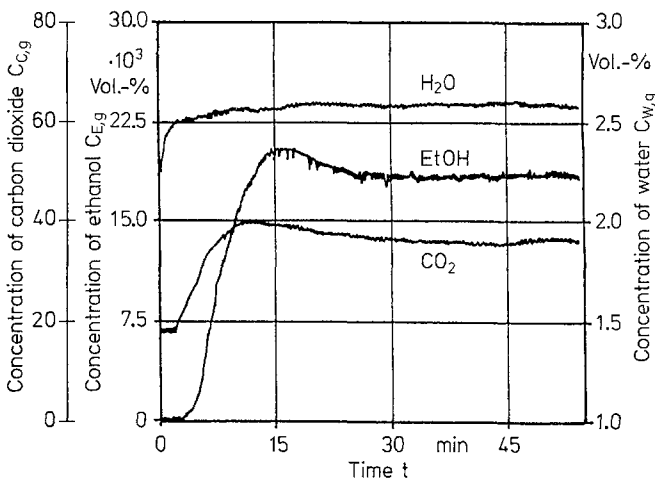


Fig. 7. Continuous gas analysis for indication of steady state in the fluid bed

and a semi-technical system, 55 cm in diameter. Figure 5 schematically shows the laboratory system. The fluidization gas had to be humidified to avoid drying and deactivation of the yeast. The fluidization behaviour was continuously monitored by an opto-electronical system [6], the composition of the fluidization gas was continuously measured by two IR-analysers. Figure 6 shows the demonstration scale fermenter. The freeboard of the reactor was isolated and heated externally to avoid condensation of water at the wall. The reaction room is conical with a volume that allows to handle 40 pounds of yeast in it.

In the fermentation experiments substrate with glucose concentrations ranging from 50–200 g/l, ammonium sulphate, yeast extract and  $\text{KH}_2\text{PO}_4$  was continuously fed to the reactor by a two phase nozzle. The temperature was varied between 20 °C–34 °C. The specific glucose flow that  $\dot{m}_{G,V}$  ranged from 19–190  $\text{kg}/(\text{m}^3 \cdot \text{h})$ . Figure 7 gives

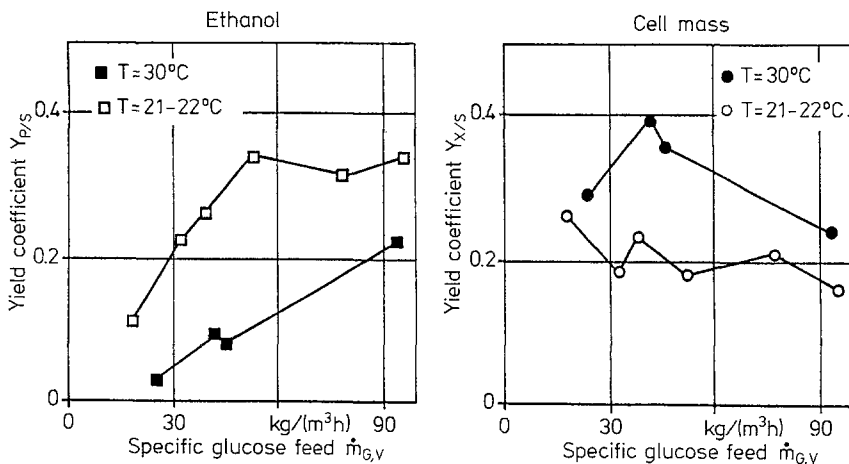


Fig. 8. Dependence of ethanol- and cell yield on specific substrate feed rate and temperature

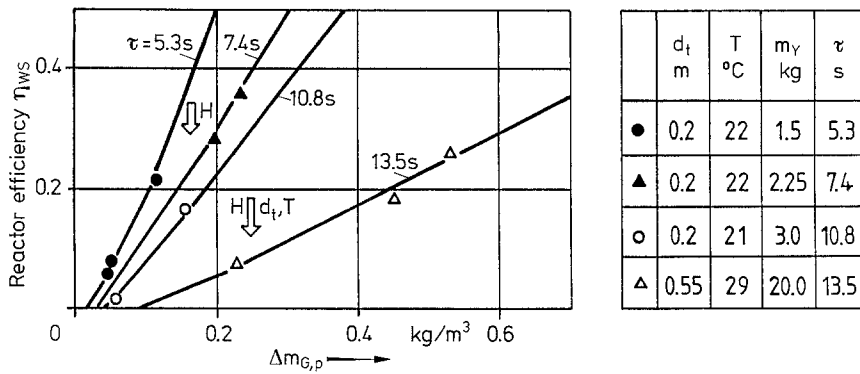


Fig. 10. Reactor efficiency for the fluidized bed gas/solid fermenter

an example for the time course of the exit gas stream composition. The initial maxima for ethanol and carbon dioxide are typical for the experiments and may be caused by a short lag phase for growth, while ethanol production start immediately. Steady state conditions were reached between 15 and 45 minutes.

4.2 Experimental yield coefficients

Yield coefficients for ethanol and carbon dioxide were calculated directly from the gas concentrations at steady state conditions. Cell yield was calculated from the increase of yeast mass at the end of the experiment. Figure 8 gives an example of experimental yield coefficients for ethanol and cell mass, measured in the laboratory scale reactor at various specific substrate feed rates and two different temperatures. It can be seen that in analogy to conventional submerged culture fermentation the ethanol yield at aerobic conditions increases strongly with increased sugar supply, i.e. higher sugar concentrations in the fluid bed, while cell yield decreases.

A raise in temperature at constant feed rates yields increasing reaction rates with a decrease of the mean sugar concentration in the bed. Therefore in this case growth reaction is dominating.

5 Comparison of experimental and theoretical yield

Figure 9 compares the yield coefficients for ethanol, cell mass and carbon dioxide of all the 14 experiments performed in both reactor types to the values predicted by the model. The difference between experimental and theoretical values seldom exceeds 20%. The proposed model seems to be appropriate to describe the reaction behaviour of a fluidized bed fermenter.

6 Reactor efficiency

For given ethanol yield, circulation time and specific substrate supply the mean specific ethanol production rate in

the fermenter  $v_{ws}$  can be calculated from Eq. (14),

$$v_{ws} = \frac{Y_{P/S}(\tau, \Delta m_{G,P}, T) \cdot \Delta m_{G,P}}{X \cdot \tau} \tag{14}$$

Dividing  $v_{ws}$  by the maximum specific reaction rate for a given temperature  $v_{max}(T)$  yields the efficiency factor of the fluid bed fermenter  $\eta_{ws}$

$$\eta_{ws} = \frac{v_{ws}}{v_{max}(T)} \tag{15}$$

Figure 10 shows the calculated reactor efficiency as a function of the specific glucose supply for three different circulation times in the laboratory scale reactor and one in the semi-technical fermenter together with experimental results.

The influence of fermenter dimensions on reactor efficiency is obvious. An increase in bed height  $H$  results in longer circulation times, which cause a decrease of reactor efficiency at limited specific glucose supply. An increase in reactor diameter  $d_t$  has the same effect. From this it is clear that an optimization of productivity for this type of fermenter can only be achieved by optimizing solids' mixing and optimal substrate distribution, to give short circulation times at maximum specific substrate supply.

References

1. Bauer, W.; Kirk, H.-G.: Untersuchungen zur Glutathion-Synthese mit *S. cerevisiae* in Solid-State- und Submersfermentation. Biotech. Forum 1985
2. Mishra, I. M.; El-Temtamy, S. A.; Schügerl, K.: Growth of *Saccharomyces cerevisiae* in Gaseous Fluidized Beds. Europ. J. Appl. Microb. Biotechnol. 16 (1982) 197–203
3. Moebus, O.; Teuber, M.; Reuter, H.: Growth of *Saccharomyces cerevisiae* in form of solid particles in a gaseous fluidized bed. Kieler Milchwirtschaftl. Forschungsber. 33 (1981)
4. Bauer, W.: Der Wirbelschichtfermenter – Entwicklung eines neuen Fermentertyps. ZFL 3 (1985) 154–161
5. Moebus, O.; Teuber, M.: Production of ethanol by solid particles of *S. cerevisiae* in a Fluidized Bed. Europ. J. Appl. Microbiol. Biotechnol. 15 (1982) 194–197

6. Bauer, W.; Röttenbacher, L.: Regelung der Substratzufuhr eines Gas/Feststoff-Wirbelschichtfermenters über die Bestimmung des Fluidisationsverhaltens. ZFL 1 (1984) 18–23
7. Rowe, P. N.: Estimation of solids circulation rate in bubbling fluidized beds. Chem. Eng. Sci. 28 (1973) 979–980
8. Röttenbacher, L.: Entwicklung und Modellierung eines Gas/Feststoff-Wirbelschichtfermenters zur Erzeugung von Ethanol mit *S. cerevisiae*. Diss. TU Hamburg-Harburg 1985

Dr.-Ing. L. Röttenbacher  
Wacker-Chemie  
D-8263 Burghausen

Dipl.-Phys. M. Schößler  
Technische Universität Hamburg-Harburg  
D-2000 Hamburg

Prof. Dr.-Ing. W. Bauer  
Fraunhofer-Institut  
für Lebensmitteltechnologie u. Verpackung  
Schrägenhofstr. 35  
D-8000 München 50  
FRG

Received March 17, 1986